CONF-860414--1

Evaluation of EBR-II Driver-fuel Elements Following an Unprotected Station Blackout Accident*

CONF-860414--1

DE86 006453

by

L. K. Chang and J. H. Bottcher
EBR-II Division

*Work supported by the U. S. Department of Energy, Reactor Systems, Development and Technology, under Contract W-31-109-Eng-38.

DISCLAIMER

Evaluation of EBR-II Driver-fuel Elements Following an Unprotected Station Blackout Accident*

Summary

One of the current design objectives for a liquid metal reactor (LMR) is the inherent shutdown-cooling capability of the reactor, such that the reactor itself can safely reduce power following a total loss of pump power without activating the reactor shutdown system (RSS). Following a loss-of-flow (LOF) accident and a failure of RSS, in EBR-II, reactor core damage and plant restartability is of considerable interest. In the LOF event, high temperature in the reactor causes negative reactivity feedback that reduces reactor power. After an accident, reactor fuel performance is one of the factors used to assess the restartability of the plant.

A thermal-hydraulic-neutronic analysis was performed to determine the response of the plant and the temperature of individual subassemblies. These temperatures were then used to assess the damage to driver fuel elements caused by the station blackout accident. The maximum depth of cladding wastage from molten eutectic at temperatures >715°C was found to be 0.0053 mm for the hottest subassembly; this value is considerably less than the 0.28 mm cladding thickness.

Introduction

Experimental Breeder Reactor II (EBR-II) is located at the Idaho National Engineering Laboratory (INEL); it is operated by Argonne National Laboratory for the U. S. Department of Energy. The plant is a sodium-cooled, pool-type fast reactor that produces a thermal power of 60 MWt and a net electrical output of about 20 MWt. EBR-II has been in operation since 1964 and has served as a fast-flux irradiation facility since 1967. Recently, the plant has also served as a operational safety test facility to demonstrate the inherently safe and reliable operation of the liquid metal reactor (LMR).

One of the major concerns in the operation of an LMR is the inherent shutdown cooling capability that can be designed into the reactor, so that the reactor can itself safely reduce power following a total loss of pumping power without activating the reactor shutdown system (RSS). A loss-of-flow (LOF) accident of considerable interest in current LMFBR studies is a station blackout coupled with a failure of the RSS. Normally, a loss of primary coolant pumping power and an increase of reactor core temperature core will set off alarms and to scram the reactor via the RSS. Should the RSS fail, the reactor temperature rise can cause negative reactivity feedback to reduce reactor power.

A shutdown heat removal testing (SHRT) program has been designed to study natural-convective-cooling phenomena and safe shutdown capability inherent in

*Work supported by the U. S. Department of Energy, Reactor Systems, Development and Technology, under Contract W-31-109-Eng-38.

EBR-II during a variety of protected (with reactor scram) and unprotected (without scram) LOF transients[1,2]. Three series of protected LOF tests and one series of reactivity feedback verification tests were performed in June of 1984 to investigate the shutdown heat removability of the plant and to characterize reactor reactivity feedback for unprotected LOF tests. In May of 1985, a series of unprotected LOF tests were performed to verify the inherent safe shutdown capability of the EBR-II plant[3,4]. In all of the tests, the peak fuel-cladding temperatures were limited by the eutectic alloy formation temperature of driver and blanket fuel elements. As a result, the initial power of all unprotected tests was limited to 16% of rated power. The measured data were used to validate the thermal-hydraulic-neutronic code, NATDEMO[5] and hot channel analysis code HOTCHAN. Good agreements between experimental measurements and analytical predictions[3,6] were achieved. In the present analysis, both NATDEMO and HOTCHAN computer codes were used for thermal predictions.

Description of the EBR-II Plant

A schematic representation of the EBR-II plant is given in Fig. 1. Since the reactor is a pool design, essentially all primary components are submerged in a large volume of sodium within the primary tank. Primary coolant flow is provided by two centrifugal pumps and an electromagnetic auxiliary pump. The rated flow of the primary system is 464 kg/s. If power should be lost to the main pumps, the auxiliary pump would provide about 5% of the rated flow.

The reactor vessel contains 16 rows of subassemblies; the inner six rows are driver subassemblies constituting the active core. Rows 7-10 are stainless steel reflector subassemblies; the outer 6 rows contain blanket subassemblies. The outlet flow from all subassemblies is well-mixed in the common reactor coolant outlet plenum. This plenum is connected to a reactor outlet pipe that routes the coolant about 12 m to the intermediate heat exchanger (IHX). The primary sodium exiting from the IHX mixes with the primary tank bulk sodium. The sodium then enters the two primary pumps, passes through about 10 m of the reactor inlet pipe and returns to the reactor. The IHX transfers the energy generated in the reactor to a secondary sodium system, and ultimately to the steam generator and turbogenerator.

Description of the Problem

During a total station blackout, there would be a simultaneous loss of pumping power to the primary and secondary systems. Electric power to the two primary pumps is supplied by a variable speed motor-generator (M-G) set for each unit. Pump motor speed is adjustable over a wide range by varying the slip of an eddy-current clutch that couples each M-G motor to the generator. Electric power is supplied to each M-G set by two pairs of circuit breakers, i.e., the 2400-volt breaker to M-G motor and a 110-volt breaker to the eddy-current clutch. Whether the auxiliary pump is on or off, the primary pumps can be tripped by (1) opening of 2400-volt and 110-volt breakers, (2) opening only the 2400-volt breakers and (3) opening only the 110-volt breakers. In the event of a total station blackout, the M-G motors and clutches will simultaneously lose power (mode 1). The primary pumps will coast to a stop in about 50 s when station blackout occurs at rated flow.

The auxiliary pump normally operates continuously and remains connected to its rectifier. During a loss of site power, the normal power supplied to the rectifier is interrupted until emergency power from a diesel/ electric unit is substituted. For the present hypothetical station blackout, a loss of both site and emergency power would be assumed and the auxiliary pump would operate only by battery. In this study the auxiliary pump is conservatively assumed to provide about 3% of rated flow when its power is supplied by the battery. The secondary system pump is also an electromagnetic type and contains no stored energy. Therefore, secondary system flow coastdown is rapid; it depends only on the initial kinetic energy of the secondary flow, and the fluid dissipation rate during the coastdown.

Analytical Approach

Certain features of the EBR-II are very important when assessing the impact of unprotected LOF transients on reactor and fuel element temperatures. It should be noted that a total loss of station power causes both the primary and secondary flow systems to coast down simultaneously. Emergency power (diesel supplied) is available to supply the primary loop auxiliary pump and to supply the main pump in the secondary loop. In addition, emergency power remains available to operate the power plant system such as steam pressure control system. In the present study the mitigating influence of these backup systems was disregarded with the result that both the primary and secondary systems experience an early transition to natural convection flow. Another important feature of the EBR-II is that it contains only metallic uranium fuel in the driver subassemblies and depleted natural uranium in the outer blanket. An intermediate zone contains 4 rows of stainless steel reflectors that enhance power generation in the driver zone. The EBR-II core characteristics cause rapid thermal response of the driver during an LOF event. Since EBR-II is a pool-type LMFBR, dynamic response of the primary-tank sodium is very slow due to the large inventory sodium in the tank; this is in strong contrast to the rapid response of the driver fuel.

The NATDEMO computer program was used for the thermal-hydraulic prediction of the EBR-II plant response; the HOTCHAN program was employed to determine the temperature of individual subassemblies. NATDEMO is a thermal-hydraulic and neutronic code specifically designed for system analysis of the EBR-II plant, as shown in Fig. 1. NATDEMO was developed to simulate the dynamic response of the plant for a variety of transients ranging from normal operation to upset conditions caused by such disturbances as flow, control rod movement, or loss of electric power. The code models 16 rows of subassemblies by dividing them into three regions; the driver fuel core, the stainless steel reflector, and the depleted uranium blanket region. Each region has a separate power generation model containing both prompt and delayed components. Fission power is derived from a point kinetics model with six delayed-neutron groups. All of three regions are described by similar thermal-hydraulic models that treat them as parallel channels with common pressure drops.

One of the important features of the NATDEMO code is its detailed model of reactivity feedback. This is essential for thermal predictions of unprotected LOF transients. Reactivity feedback in EBR-II is all negative except the subassembly bowing component which can vary from positive to negative depending upon reactor loading and power and flow distribution. A detailed

description of EBR-II reactivity feedback components is given in ref. 7. Although a post test analysis indicates that the reactivity feedback components of bowing are positive for the reactivity feedback verification tests of June 1984[7], the bowing contribution was not considered in the present work because of core loading and subassembly bowing behavior uncertainties.

NATDEMO was used to predict the whole reactor plant and to provide information on the thermal and hydraulic environment in the driver region. This information was used in the HOTCHAN code to predict the temperature of the individual subassemblies. The input required for the HOTCHAN hot channel analysis includes the transient-neutronic and gamma powers, the pressure drop across the core, and the average temperature profile of the surrounding subassemblies. HOTCHAN is capable of predicting the temperature of either a standard 91-element driver or a 61-element control rod, including the thimble flow region. The driver subassembly was radially divided into three regions to represent the 91-element driver subassembly; while in the case of the 61-element control rod subassembly, two regions were modeled to represent the fuel elements, and/or simulate the thimble flow area. The HOTCHAN model is axisymmetric; it has a transient thermal-boundary condition to allow intersubassembly heat transfer predictions within a cluster of seven subassemblies.

Thermal-hydraulic-neutronic Response of the Reactor

During a total station blackout, a transient would be initiated by simultaneously tripping the 2400-volt M-G breakers and the 110-volt clutch breakers at the primary and secondary pumps. The auxiliary pump rectifier would also be tripped so that the auxiliary pump is operated on battery only. When the primary pump is tripped, the reactor temperature rises due to the loss-of-flow. The resulting high temperature in the core causes negative reactivity feedback and consequently reduces reactor power. The normalized reactor power and flow are given in Fig. 2, and the transient excess reactivity is depicted in Fig. 3. The minimum excess reactivity corresponds to maximum core temperature. The average driver subassembly sodium temperature at the top of the core and at the subassembly outlet are shown in Fig. 4. This indicates that the sodium temperature of the driver increases rapidly as flow coasts down. A natural convective flow increase and a power decrease causes the temperature to decrease after the peak has been reached. The coolant temperature at the driver-fuel subassembly outlet is lower than that at the top of the core and its peak occurs later. This is caused by the low flow rate as flow coastdown proceeds, and also by the heat capacitance effect of sodium and subassemblies. The reactor sodium mixed-mean temperatures at the reactor plenum inlet and outlet are considerably lower than those plotted in Fig. 4. This is caused by slow flow transport and the mixing and heat capacitance effect in the reactor outlet plenum. Thermal responses of the balance of the plant is mild; the reactor inlet temperature remains almost constant during the first 300 s of the transient.

Temperatures of Driver Subassemblies

The reactor loading of EBR-II varies from run to run, and the temperatures of individual driver subassemblies may change as well. In the present analysis, the proposed reactor loading for run 129D loading was used for the

evaluation. For run 129D the core contains 65 driver subassemblies, 8 half-worth drivers and several of experimental fuel and structural subassemblies. Two instrumented subassemblies, XX09 and XX10, are in row 5 control rod positions 5D3 and 5C1, respectively. A standard driver subassembly contains 91 Mark-II fuel elements; instrumented subassembly XX09 and the control rods contain 61 Mark-II fuel elements. A standard half-worth driver contains approximately half Mark-II fuel elements and half stainless steel elements. The analysis indicated that the hottest subassembly during a steady-state condition may not have the highest temperature during a transient. If two subassemblies have the same initial temperature, the subassembly with the highest initial power will have the highest temperature during the transient. The hot drivers can be identified from the subassembly steady-state powers and temperatures except for row 6 which contains both high-flow and low-flow subassemblies. All of the drivers in each row are expected to have the same flow rate, therefore, the subassembly with the highest initial power will have the highest temperature during a transient.

The NATDEMO calculations simulate the thermal-hydraulic environment of the driver region. This information was used in the HOTCHAN code to predict transient temperatures of 91 and 61 element subassemblies. The hottest subassembly was identified as a 91-element driver subassembly in row 4; the peak cladding temperature of this subassembly is 842°C. Fuel element damage is not expected when the fuel-cladding temperature is below the eutectic alloy formation temperature of 715°C. Fuel-cladding damage is a function of the time that the cladding remains above the eutectic alloy formation temperature. Table I lists the subassemblies with cladding temperatures above the eutectic point, along with the time the cladding stays above the eutectic temperature. This information was used to perform a fail-safe evaluation of the driver subassemblies in the EBR-II core.

Evaluation of Driver Fuel Elements

The EBR-II driver-fuel element (Mark-II) is composed of an uranium-5 wt % fissium* metal fuel pin that is sodium bonded (for heat transfer) to stainless steel cladding. The design is shown in Fig. 5 and described in detail in Table II.

With this fuel element design the major consequence of the high temperatures encountered during a LOF accident would be the formation of low-melting-point alloys of fuel and cladding that can degrade operating performance of the elements. The eutectic alloy is an uranium 34 wt % iron alloy. The eutectic temperature for formation of this liquid alloy is 715 ± 5°C.[8] At or above this temperature, iron readily diffuses into the fuel while uranium diffuses into the cladding to form a liquid eutectic alloy and other intermetallic compounds. This phenomenon reduces the effective thickness of the cladding, and with sufficient exposure may lead to cladding failure.

*Fissium is an equilibrium concentration of fission-product elements left by the pyrometallurgical reprocessing cycle designed for EBR-II and consists of 2.4 wt % molybdenum, 1.9 wt % ruthenium, 0.3 wt % rhodium, 0.2 wt % palladium, 0.1 wt % zirconium, and 0.01 wt % niobium.

TABLE I. Peak Fuel-cladding Temperature and Damages of Driver Subassemblies

Range of Peak Fuel Cladding Temperatures, °C	No. of Subassemblies in the Temperature Range		Estimated Time Staying Above Eutectic Temperature, s	Cladding Wastage m x 10^{-6}
	Driver	Safety/Control Rod		
715-730	2	0	5	<0.1
731-745	0	2	10	0.2
746-760	3	0	15	0.6
761-790	15	3	30	1.8
791-815	30	4	50	5.0
816-845	15	0	60	10.6

TABLE II. Design Parameters of Mark-II Fuel Elements

	Mark-II
Enrichment weight, % ^{235}U	67
Fuel-pin weight, g	52
Fuel-pin length, in.	13.5
Fuel-pin diameter, in.	0.130
Fuel/cladding bond	Sodium
Fuel/cladding radial gap, in.	0.010
Cladding-wall thickness, in.	0.012
Cladding-wall OD, in.	0.174
Length, in.	24.1
Restrainer height above fuel, in.	0.500
Sodium level above fuel, in.	1.25
Plenum volume, $in.^3$	0.147
Plenum gas	Argon
Cladding material	316
Spacer-wire diameter, in.	0.049
Spacer-wire material	316

Cladding wastage is a direct measure of the diffusion processes that control the eutectic alloy formation rate. These processes are governed by the diffusivities of uranium and iron, and their respective exponential temperature dependence. Several studies have reported this type of eutectic alloy formation and the wastage, or penetration rate of molten fuel on unirradiated stainless steel or iron cladding.[8-10] Results of these studies shows that the wastage rate has an exponential temperature dependence for temperatures <1080°C which is shown in Fig. 6. Figure 6 gives a plot of molten eutectic alloy penetration into iron as a function of temperature.[10] The correlation for this wastage rate ($\dot{w}$) may be expressed as follows:

$$\dot{w} = 4.1 \times 10^{-9}\ e^{0.02T},\ T = \text{temperature}\ (730 < T < 1080°C).$$

$$\dot{w} = \mu m/s$$

This correlation for unirradiated iron is conservative compared to the limited low-temperature data from stainless steel wastage studies.[8,9]

However, under in-reactor conditions, the Mark-II fuel element cladding wastage will be enhanced by the fluence accumulation. This is caused by the increased lattice-defect concentration,[11] which is reflected in volume swelling, that increases the effective diffusivity of uranium and iron. At the end-of-life condition, the cladding wastage for the same temperature and time conditions, may be enhanced by a factor of two. Using the above correlation, the calculated wastage of type 316 stainless steel enhanced by two for the peak temperature condition of each temperature range and time period (listed in Table I). These results were then multiplied by the factors two and are listed in the last column of Table I.

The ultimate impact of eutectic-induced cladding wastage, is cladding failure. This impact was studied by heating Mark-II fuel elements with a fuel burnup of 7.8 at. % to 750, 800, and 850°C and holding this temperature until cladding failure occurred.[12] The results of this out-of-pile study showed that the time to failure was shorter than the time required to completely waste the cladding. This was true particularly for higher burnup elements. However, there are many other factors that influence the time-to-failure for these fuel elements. The primary factor is cladding hoop stress caused by fission gas production during irradiation. Other factors are irradiation enhanced uranium and iron diffusion, and the presence of an interdiffusional zone to ~ 5μm thick that develops during normal operation.

Based on the Mark-II fuel element eutectic-induced cladding failure tests, the calculated time to failure at a 845°C peak temperature would be 780 seconds at the beginning-of-life, or 230 seconds at the end-of-life. This is much longer than the peak 60 second period above the eutectic temperature (Table I). Cladding failure caused by eutectic alloy wastage would not be anticipated in the LOF event described herein.

The real impact of this LOF event will be on the subsequent steady-state fuel element performance. It appears reasonable to assume that the impact would be negative even though, under normal conditions, the eutectic alloy is in the solid state. There have not been any performance studies made using Mark-II fuel elements with eutectic induced wastage. It is likely from a metallurgical point of view that in the solid-state eutectic alloy, now

composed of U_6Fe and UFe_2 intermetallics, would structurally and chemically compensate for some of the wasted cladding.

Conclusion

During an unprotected LOF accident analyzed in EBR-II, fuel elements in about 80% of the driver subassemblies would be damaged. The depth of cladding penetration will range from 1.0×10^{-5} to 1.06×10^{-2} mm. These values are considerably less than the thickness of the 0.28 mm, cladding; it would therefore be possible to restart the plant after an LOF without scram accident.

This study also notes that the feedback reactivity due to thermal bowing is not considered. Even with 2.5¢ positive bowing used in this calculation, as indicated in ref. 7, the peak cladding temperature of the hottest element will be 875°C. For this temperature the corresponding maximum cladding penetration is 2.0×10^{-2} mm, which is considerably less than the cladding thickness and should not cause cladding failure.

Recently, the EBR-II primary pumps have been modified to increase the pump coastdown time during a loss-of-pumping-power event. For a station blackout, the 110-volt power to the primary pump M-G set clutch will be on the protected, battery-backed power supply. Therefore, the primary pump coastdown time is about 100 s, which is considerably longer than the ~ 50 s coastdown time used in this analysis. In other words, the reactor temperature is expected to be lower than the present calculations indicate.

References

1. R. M. Singer et al., "Dynamic Heat Removal and Dynamic Plant Testing at EBR-II," Proceeding of the Second Specialists' Meeting on Decay Heat Removal and Natural Convection in LMFBRs, April 17-19, 1985, Long Island, New York.

2. H. P. Planchon et al., "The Experimental Breeder Reactor II Inherent Shutdown and Heat Removal Tests - Test Results and Analysis," International Topical Meeting on Fast Reactor Safety, April 21-25, 1985, Knoxville, Tenn.

3. L. K. Chang et al., "An Experimental and Analytical Investigation of Unprotected Loss-of-Flow Events in EBR-II," Am. Nucl. Soc. Tran., Vol. Nov. 1985.

4. H. P. Planchon et al., "The EBR-II Shutdown Heat Removal Testing Program: Results and Plans," Am. Nucl. Soc. Tran., Vol. , Nov. 1985.

5. D. Mohr and E. E. Feldman, "A Dynamic Simulation of the EBR-II Plant During Natural Convection with NATDEMO Code," Decay Heat Removal and Natural Convection in Fast Breeder Reactors, Hemisphere Publication Corp. (1981), pp. 207-223.

6. L. K. Chang et al., "Experimental and Analytical Study of Loss-of-Flow Transients in EBR-II Occurring at Decay Power Levels," 7th Miami International Conference on Alternate Energy Sources, December 9-11, 1985, Miami Beach, Florida.

7. D. Mohr and L. K. Chang, "Perturbation of Reactor Flow and Inlet Temperature for Reactivity Feedback Validation," International Topical Meeting on Fast Reactor Safety, April 21-25, 1985, Knoxville, Tenn.

8. C. M. Walters and L. R. Kelman, "Penetration Rate Studies of Stainless Steel by Molten Uranium and Uranium-Fissium Alloy," J. Nucl. Mat. 6(3), pp. 281-290 (1962).

9. C. M. Walters and C. E. Dickerman, "TREAT Study of the Penetration of Molten Uranium and U/5 wt % Fs Alloy through Type 304 Stainless Steel," Nucl. Sci. and Eng. 18, pp. 518-524 (1964).

10. C. M. Walters and L. R. Kelman, "The Interaction of Iron with Molten Uranium," J. of Nucl. Mat. 20, (1966) pp. 314-322.

11. E. R. Gilbert, "In-reactor Creep of Reactor Materials," Reactor Tech. 1971, Vol. 14-3, pp. 258-284.

12. P. R. Betten, J. H. Bottcher, and B. R. Seidel, "Eutectic Penetration Induced Cladding Rupture in EBR-II Driver Fuel Element," Trans. Am. Nucl. Soc. 45, pp. 300-301, Oct. 1983.

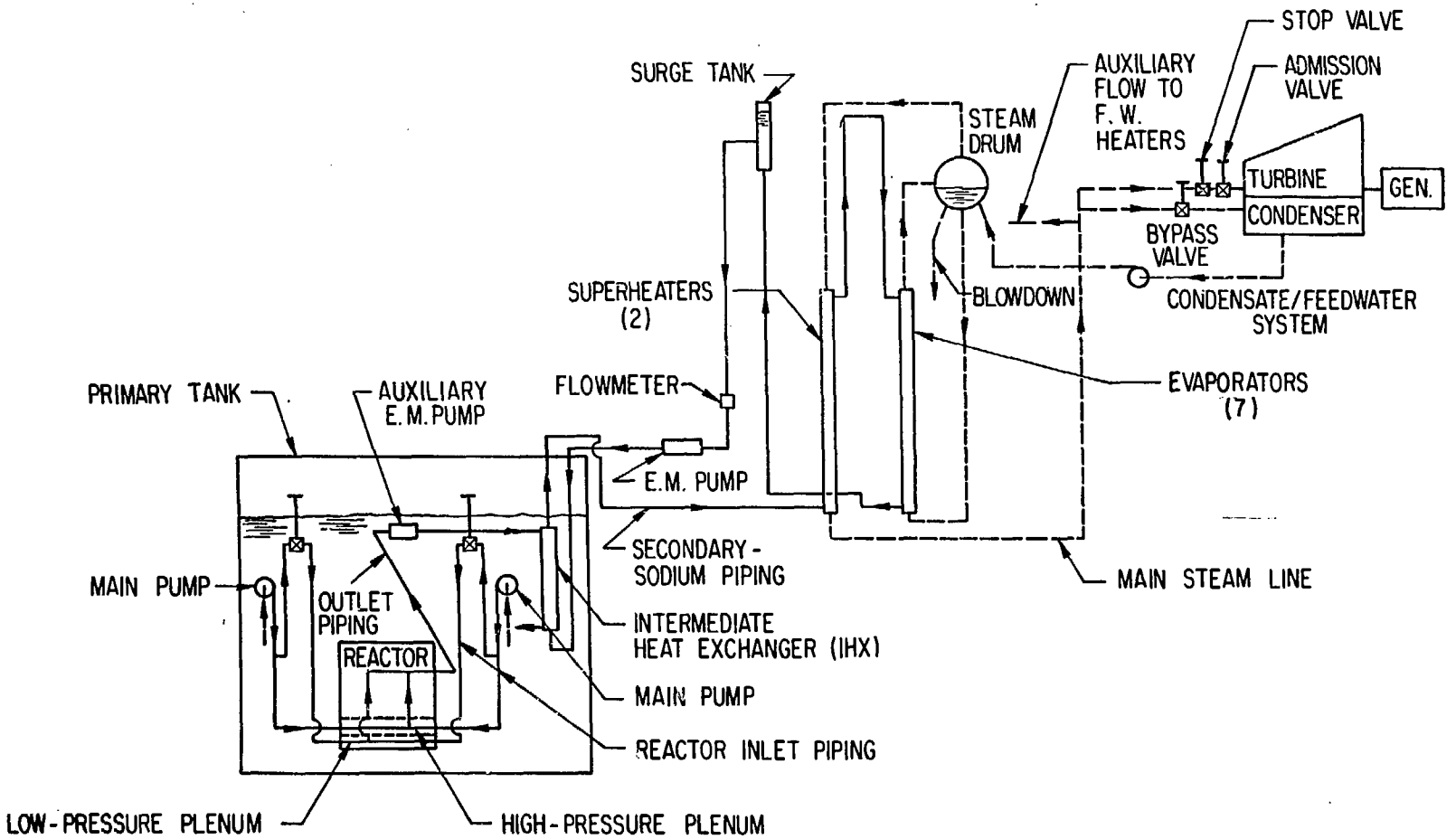

Fig. 1. Schematic Representation of the EBR-II Plant

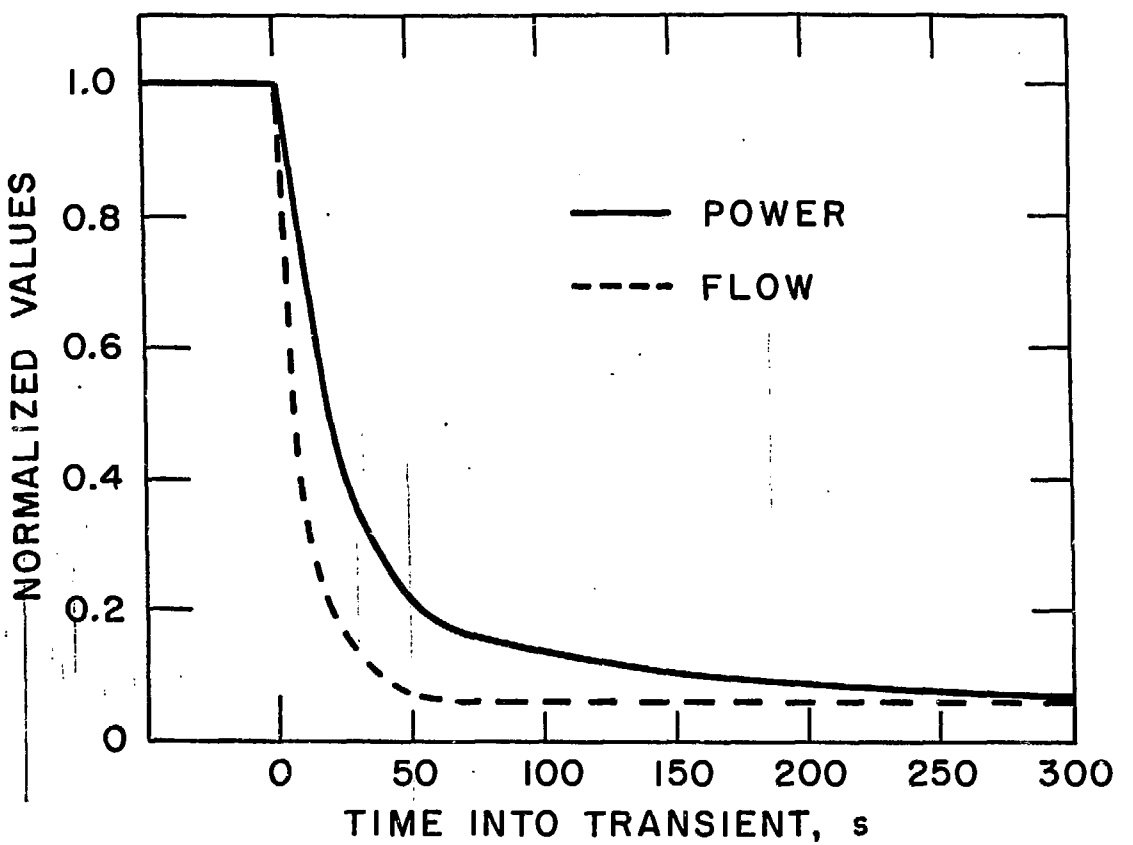

Fig. 2. Reactor Power and Flow Response during Transient

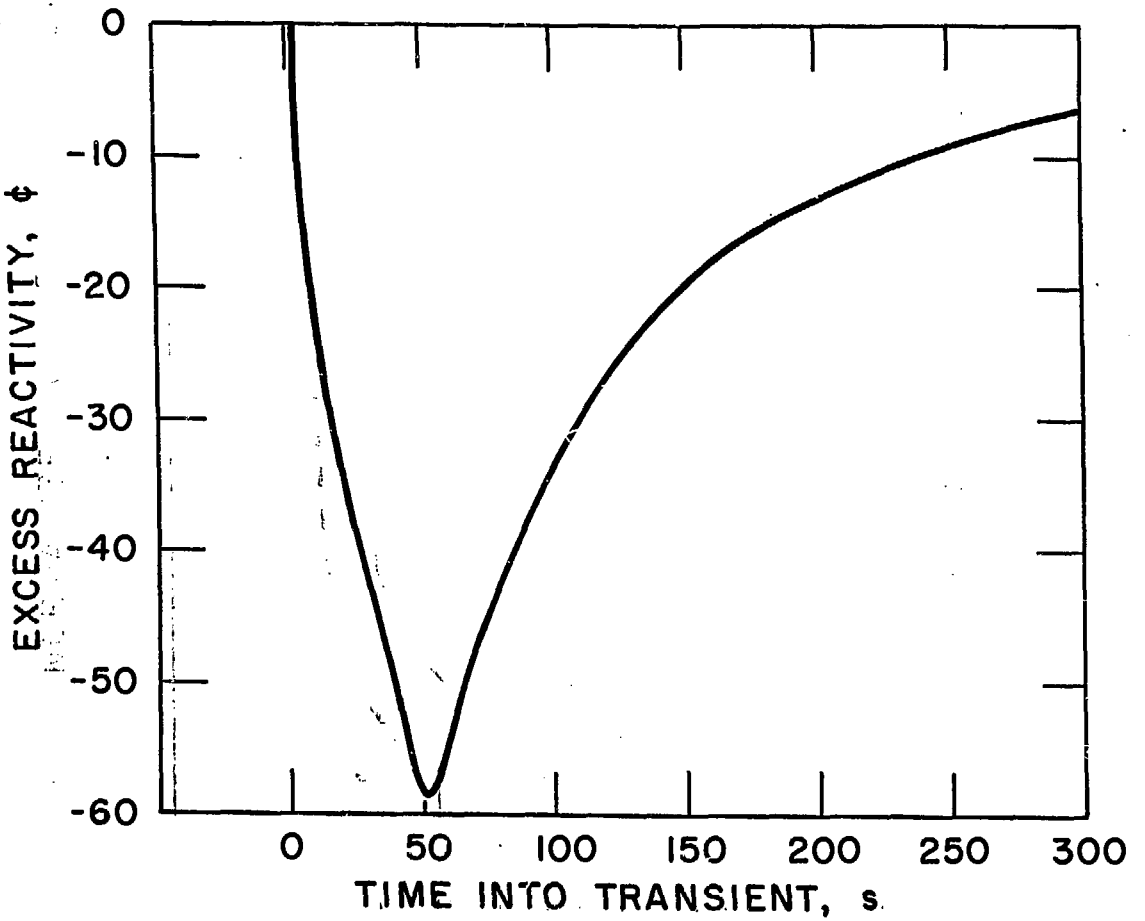

Fig. 3. Excess Reactivity during Transient

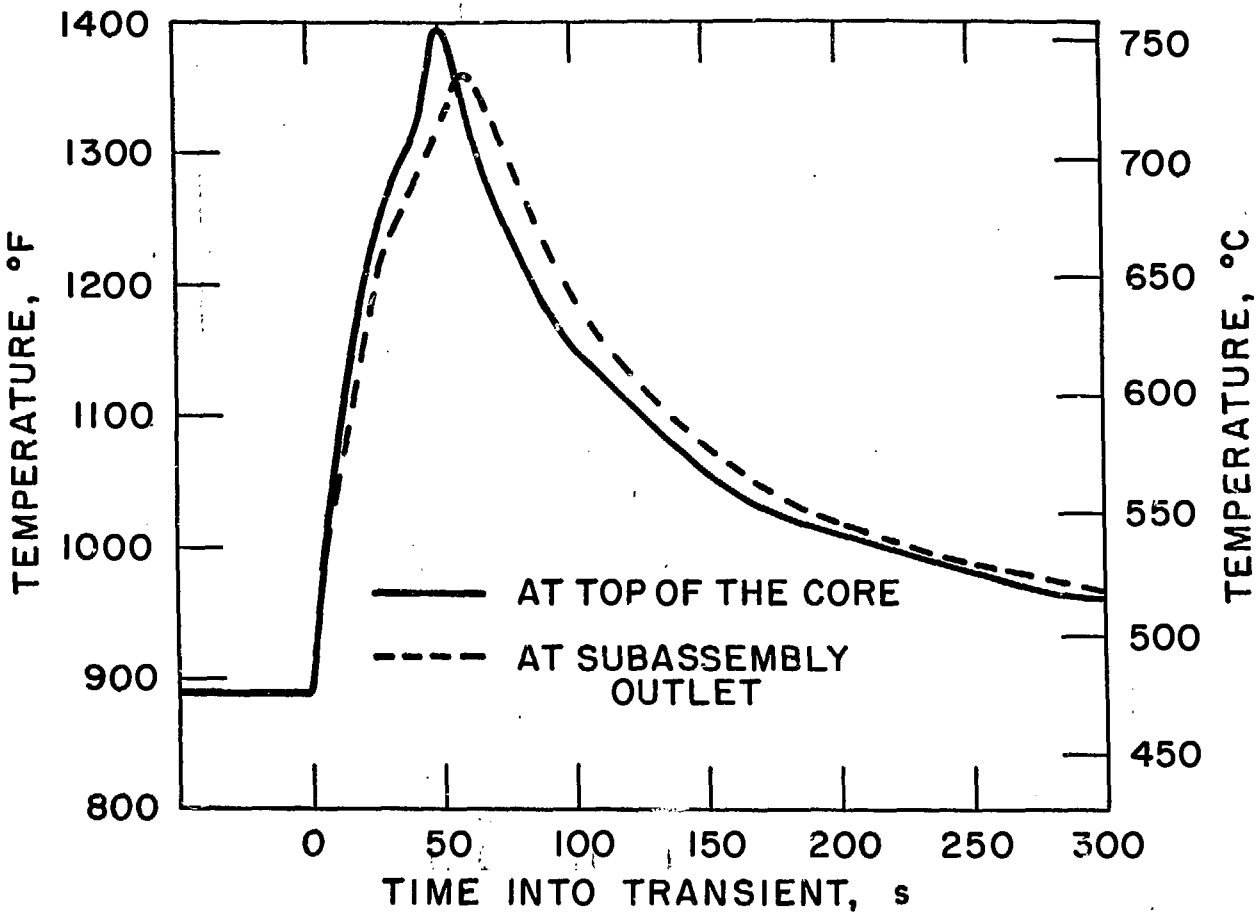

Fig. 4. Transient Driver Temperature Response

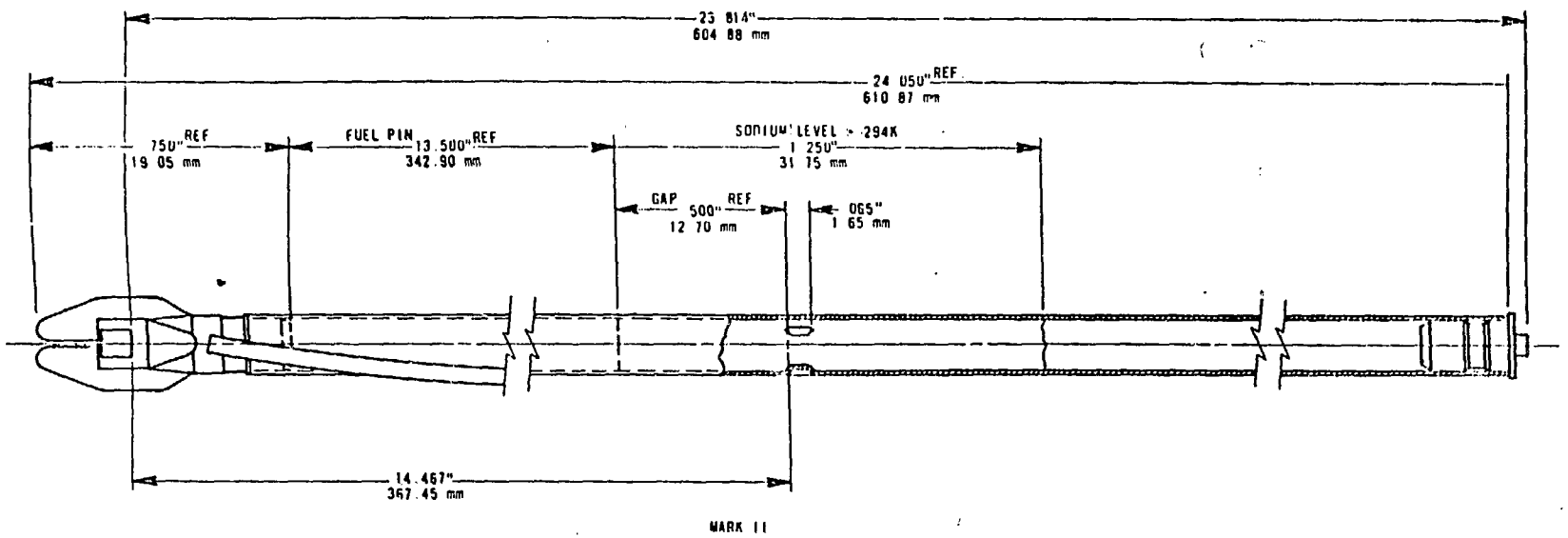

Fig. 5. EBR-II Driver Fuel Element (Mark-II)

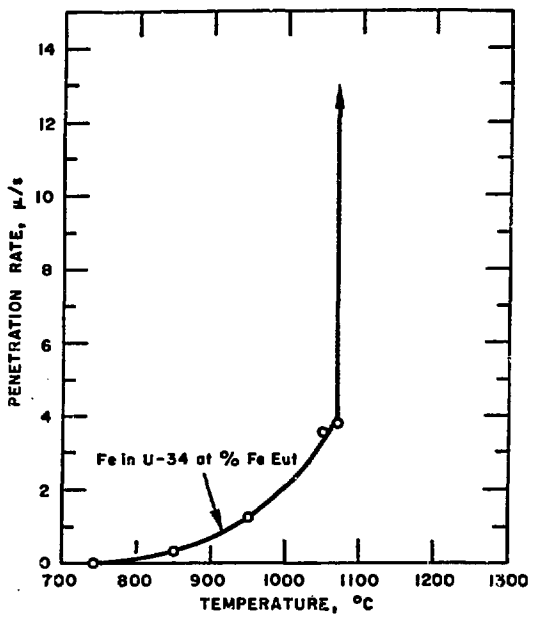

Fig. 6. Penetration Rate of the Stainless Steel Cladding